

Assemblies of Redox-Active Metallodendrimers Using Hydrogen Bonding for the Electrochemical Recognition of the H_2PO_4^- and Adenosine-triphosphate (ATP^{2-}) Anions

Marie-Christine Daniel, Fatou Ba, Jaime Ruiz Aranzas, and Didier Astruc*

Molecular Nanosciences and Catalysis Group, LCOO, UMR CNRS No. 5802, Université Bordeaux I, 33405 Talence Cédex, France

Received May 7, 2004

Two families of five metallodendrimers have been assembled by hydrogen bonding between the primary amino groups of DSM dendrimers G_n -DAB-dendr-(NH_2) $_x$ ($n = 1-5$; $x = 4, 8, 16, 32, 64$) and the OH group of phenol dendrons containing a triallyl or a triferrocenylalkyl tripod in para position. These H-bonded dendrimers noted G_1 -DAB-12Fc, G_2 -DAB-24Fc, G_3 -DAB-48Fc, G_4 -DAB-96Fc, and G_5 -DAB-192Fc have been characterized as resulting from fast, reversible hydrogen bonding by the single broad signal observed in ^1H NMR for the three $\text{NH}_2 + \text{OH}$ protons whose location depends on the concentration. The cyclic voltammograms (CVs) show a single reversible ferrocenyl wave due to the equivalence of these groups and the fast rotation of the supramolecular ensemble compared to the CV time scale. A new CV wave appears at less anodic potential upon addition of H_2PO_4^- or adenosine-triphosphate (ATP^{2-}) anion as a tetrabutylammonium salt as with previously studied ferrocenyl dendrimers. In addition, other specific and remarkable features are the fact that the new CV wave is much less intense than the initial one and the dramatically sudden disappearance of the initial CV wave at the equivalent point indicating the formation of a large supramolecular assembly with the hydrogenophosphate groups. Finally, the variation of the number of equivalent anions with the generation number to reach the equivalent point also suggests that the competition between the amino- and amido group for the interaction with hydrogenophosphate depends on the generation number. Recognition by these supramolecular dendrimers of H_2PO_4^- and ATP^{2-} follows the model of the relatively strong-interaction type in the Kaifer–Echegoyen model, which allows access to the ratio of association constants K_+/K_0 . A positive dendritic effect is found for the recognition of H_2PO_4^- (i.e., the difference of potentials $\Delta E_{1/2}$ between the initial CV wave and the new one and the K_+/K_0 value increase as the generation number increases) whereas the dendritic effect is slightly negative for the recognition of ATP^{2-} .

Introduction

Recognition and sensing of anions is of crucial importance viewing their role in the biological, pharmaceutical, and environmental contexts. Endo-receptors¹ to which a redox-active metallocenyl fragment is attached have been largely developed by Beer and his group.² Subsequently, we have

investigated exo-receptors³ based on dendrimers⁴ and dendronized gold nanoparticles.^{3d,3e} The synthetic efforts in these studies are noteworthy and may be considered as a limiting factor. Therefore, we have sought dendritic exo-receptors that are reversibly assembled in a more simple, supramolecular way using hydrogen bonding.⁵ It is known that simple alcohols and primary amines form complementary O- -H- -N bonds with tetrahedral disposition of both O and N atoms and 1:1 stoichiometry (Figure 1),⁵ a property that has been astutely used in crystal engineering^{5c} and chiral recognition.^{5d}

* Author to whom correspondence should be addressed. E-mail: d.astruc@lcoo.u-bordeaux1.fr.

- (1) Lehn, J.-M. *Supramolecular Chemistry: Concepts and Perspectives*; VCH: Weinheim, 1995.
 (2) (a) Beer, P. D. *Adv. Inorg. Chem.* **1992**, *39*, 79. (b) Beer, P. D.; Drew, M. G. B.; Hodacova, J.; Stokes, S. E. *J. Chem. Soc., Dalton Trans.* **1995**, 3447. (c) Beer, P. D. *J. Chem. Soc., Chem. Commun.* **1996**, 689. (d) Beer, P. D. *Acc. Chem. Res.* **1998**, *31*, 71. (e) Beer, P. D.; Gale, P. A.; Chen, Z. *Adv. Phys. Org. Chem.* **1998**, *31*, 1. (f) Beer, P. D.; Gale, P. A. *Angew. Chem., Int. Ed.* **2001**, *40*, 486. (g) Beer, P. D.; Davis, J.; Drillsma-Millgrom, D. A.; Szemes, F. *Chem. Commun.* **2002**, 1716.

- (3) (a) Valério, C.; Fillaut, J.-L.; Ruiz, J.; Guittard, J.; Blais, J.-C.; Astruc, D. *J. Am. Chem. Soc.* **1997**, *119*, 2588. (b) Labande, A.; Ruiz, J.; Astruc, D. *J. Am. Chem. Soc.* **2002**, *124*, 1782. (c) Valério, C.; Alonso, E.; Ruiz, J.; Blais, J.-C.; Astruc, D. *Angew. Chem., Int. Ed.* **1999**, *38*, 1747. (d) Daniel, M.-C.; Ruiz, J.; Nlate, S.; Blais, J.-C.; Astruc, D. *J. Am. Chem. Soc.* **2003**, *125*, 2617. (e) Daniel, M.-C.; Astruc, D. *Chem. Rev.* **2004**, *13*, 293.

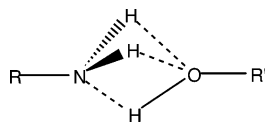


Figure 1.

In a preliminary communication,⁶ we reported the recognition and titration of H_2PO_4^- by dendrimers assembled using DSM's DAB polyamines^{7,8} with phenols containing a triferrocenylalkyl tripod in para position.^{3d} We have now extended this study to the biologically important anion ATP^{2-} that is one of the four DNA nucleotides and the source of bioenergy for cells.⁹ We find that it can also be recognized and titrated by these supramolecular dendrimers and report here these studies in detail in which the recognition and titration of H_2PO_4^- and ATP^{2-} are compared. Although the anion H_2PO_4^- has been the subject of various recognition studies,^{3,4} ATP^{2-} has so far been examined little from this point of view.¹⁰ Supramolecular aspects of dendrimers have already been developed, in particular by the groups of Newkome,¹¹ Zimmermann,¹² and Meijers,¹³ although the present study is the first one devoted to electrochemical sensing using H-bonded dendrimers.

Results

Given the known ability of primary amines to form hydrogen bonds with alcohols,⁵ we have assembled functionalized phenols with the commercial DSM DAB den-

drimers of generation 1–5 containing 4–64 NH_2 groups.⁷ The phenols are dendronic bricks with the phenol function at the focal point and three terminal double bonds or amidoferrocenyl groups at the extremities of the tripod branches.¹⁴ All the assemblies were performed by mixing equivalent amounts of phenol and amino groups. The primary amines alone form intermolecular hydrogen bond as shown by the presence of a very broad infrared band around 3500 cm^{-1} , and the addition of a phenol does not bring about a significant change, but ^1H NMR is informative.

NMR. The solutions of H-bonded dendrimers were prepared in CDCl_3 to allow the characterization by ^1H NMR. Indeed, upon mixing, the NH_2 and OH protons appear as a unique and broad common signal located between 2.4 and 4.1 ppm depending on the concentration. By comparison with the free phenols and DAB polyamine dendrimers, the phenol proton is shielded and the amine protons are deshielded in the supramolecular dendritic assembly. The comparison of the triallylphenol–DAB and triferrocenylphenol–DAB mixtures allows a better understanding of the ^1H NMR events, since the ferrocenyl-free dendron does not hide the OH region whereas the ferrocenyl groups do. For instance, Figure 2 shows the ^1H NMR spectra of free and assembled triallylphenol and G_3 -dendr-DAB-(NH_2)₁₆. The new signal reflects the hydrogen-bond formation that is reversible and faster than the NMR time scale, and the equivalency of these three $\text{NH}_2 + \text{OH}$ protons.

A representation of the assembly between the triferrocenylphenol dendron and DAB dendrimers is shown in Figures 3 and 4. The NMR spectra indicate that the system is H-bonded with fast equilibrium between the hydrogen-bonded and free forms (Figures 5 and 6) as shown by the shift of the $\text{NH}_2 + \text{OH}$ signals typical of hydrogen-bonded systems when the concentration is changed.

Cyclic Voltammetry. The cyclic voltammograms (CV) recorded in dichloromethane solution with the hydrogen-bonded dendrimers for the five generations G_1 – G_5 show a single CV wave that is chemically and electrochemically reversible at $25\text{ }^\circ\text{C}$ without adsorption except with G_5 . For G_5 , DAB-192Fc shows a slight adsorption characterized by $\Delta E_p = 45\text{ mV}$ instead of the classic 58 mV value for reversible one-electron systems. The $E_{1/2}$ values, recorded vs. Ag/AgCl are gathered in Table 1.

Electrochemical recognition and titration of the oxoanions H_2PO_4^- and ATP^{2-} . H_2PO_4^- . The addition of $[\text{H}_2\text{PO}_4][n\text{-Bu}_4\text{N}]$ to a solution of one of the supramolecular

- (4) For recent reviews on dendrimers (a) and metalodendrimers (b) see the following. (a) Newkome, G. R.; Moorefield, C. N.; Vögtle, F. *Dendrimers and Dendrons: Concepts, Synthesis and Applications*; VCH–Wiley, Weinheim, 2001. *Dendrimers and other Dendritic Polymers*; Tomalia, D., Fréchet, J. M. J., Eds.; Wiley-VCH: New York, 2002. *Dendrimers and Nanosciences*; Astruc, D., Ed.; Elsevier: Paris, 2003, Vol. 8–10. Matthews, O. A.; Shipway, A. N.; Stoddart, J. F. *Prog. Polym. Chem.* **1998**, 23, 1. Smith, D. K.; Diederich, F. *Angew. Chem. Eur. J.* **1998**, 4, 1353. Hecht, S.; Fréchet, J. M. J. *Angew. Chem., Int. Ed.* **2001**, 40, 74. (b) Newkome, G. R.; He, E.; Moorefield, C. N. *Chem. Rev.* **1999**, 99, 1689. Bosman, A. W.; Jansen, E. W.; Meijers, E. W. *Chem. Rev.* **1999**, 99, 1665. Cuadrado, I.; Morán, M.; Casado, Alonso, B.; Losada, J. *Coord. Chem. Rev.* **1999**, 189, 123. Hearshaw, M. A.; Moss, J. R. *Chem. Commun.* **1999**, 1. Astruc, D.; Chardac, F. *Chem. Rev.* **2001**, 101, 2991.
- (5) (a) For a seminal article on the complementary H-bonding between alcohol and amines, see the following. Ermer, O.; Eling, A. *J. Chem. Soc., Perkin Trans. 2* **1994**, 925. (b) Melwyn-Hugues, E. A. *Physical Chemistry*, 2nd Ed., Pergamon: Oxford, 1961; p 1060. (c) Desiraju, G. R. *Crystal Engineering: The Design of Organic Solids*; Elsevier: New York, 1989. (d) Hanessian, S.; Simard, M.; Roelens, S. *J. Am. Chem. Soc.* **1995**, 117, 7630. (e) For early reports, see the following. Lamberts, L. Z. *Phys. Chem.* **1970**, 92, 5347. Arnett, E. M.; Mitchell, E. J.; Murty, T. S. S. R. *J. Am. Chem. Soc.* **1974**, 96, 3875.
- (6) Daniel, M.-C.; Ruiz, J.; Astruc, D. *J. Am. Chem. Soc.* **2003**, 125, 1150.
- (7) de Brabander-van den Berg, E. M. M.; Meijer, E. W. *Angew. Chem., Int. Ed. Engl.* **1993**, 32, 1308.
- (8) Daniel, M.-C.; Ruiz, J.; Daro, N.; Astruc, D. *Chem. Eur. J.* **2003**, 9, 4371.
- (9) Rawn, J. D. *Biochemistry*; Neil Patterson: Burlington, NC, 1989. Ingraham, L. L.; Pardee, A. B. Free energy and entropy in metabolism. In *Metabolic Pathways*; Greenberg, D. M., Ed.; Academic Press: New York, 1967; Vol. 1.
- (10) For previous studies on recognition of ATP^{2-} by a mononuclear ferrocenyl derivative, see (a) Beer, P. D.; Cadman, J.; Lloris, J. M.; Martínez-Máñez, R.; Padilla, M. E.; Pardo, T.; Smith, D. K.; Soto, J. *J. Chem. Soc., Dalton Trans.* **1999**, 127. (b) Reynes, O.; Maillard, F.; Moutet, J.-C.; Royal, G.; Saint-Aman, E.; Stanciu, G.; Dutasta, J.-P.; Gosse, I.; Mulatier, J.-C. *J. Organomet. Chem.* **2001**, 637–639, 356. (c) Reynes, O.; Moutet, J.-C.; Pecaut, J.; Royal, G.; Saint-Aman, E. *New J. Chem.* **2002**, 26, 9.

- (11) Newkome, G. R.; Woosley, B. D.; He, E.; Moorefield, C. N.; Guther, R.; Baker, G. R.; Escamilla, G. H.; Merrill, J.; Lufmann, H. *Chem. Commun.* **1996**, 2737.
- (12) (a) Zimmerman, S. C.; Zeng, F.; Reichert, D. E. C.; Kolotuchin, S. V. *Science* **1996**, 271, 1095. (b) Wang, Y.; Zeng, F.; Zimmermann, S. C.; *Tetrahedron Lett.* **1997**, 38, 5459. (c) Zeng, F.; Zimmermann, S. C. *Chem. Rev.* **1997**, 97, 1681.
- (13) (a) Jansen, J. F. G. A.; de Brabander-van den Berg, E. M. M.; Meijer, E. W. *Science* **1994**, 265, 1226. (b) Jansen, J. F. G. A.; Meijer, E. W. *J. Am. Chem. Soc.* **1995**, 117, 4417.
- (14) (a) Sartor, V.; Djakovitch, L.; Fillaut, J.-L.; Moulines, F.; Neveu, F.; Marvaud, V.; Guittard, J.; Blais, J.-C.; Astruc, D. *J. Am. Chem. Soc.* **1999**, 121, 2929. (b) Ruiz, J.; Lafuente, G.; Marcen, S.; Ornelas, C.; Lazare, S.; Cloutet, E.; Blais, J.-C.; Astruc, D. *J. Am. Chem. Soc.* **2003**, 125, 7250.

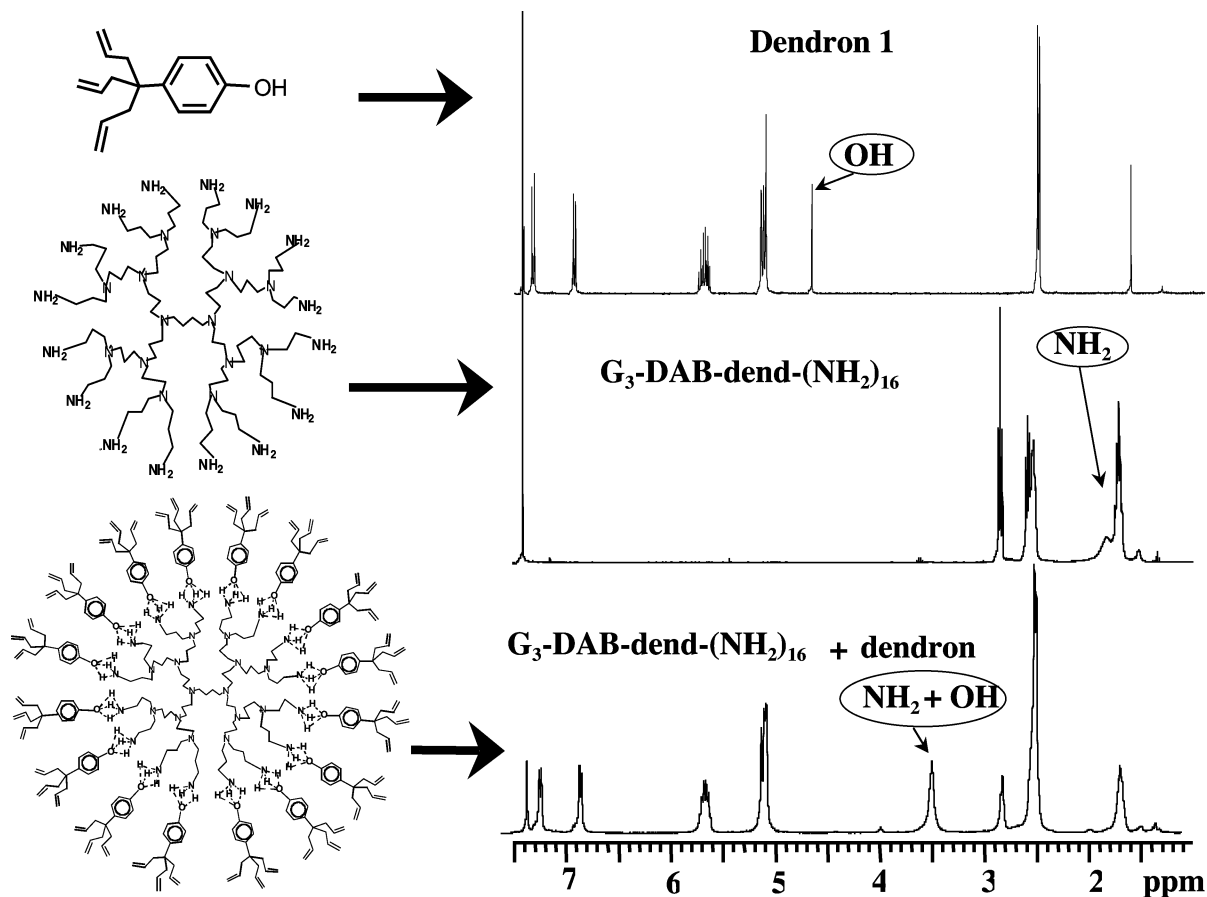


Figure 2. ^1H NMR spectra (400 MHz) of the dendron $p\text{-(CH}_2\text{=CHCH}_2\text{)}_3\text{C-C}_6\text{H}_4\text{OH}$, **1**, $\text{G}_3\text{-DAB-dend-(NH}_2\text{)}_{16}$, and of their assembly by hydrogen bonding.

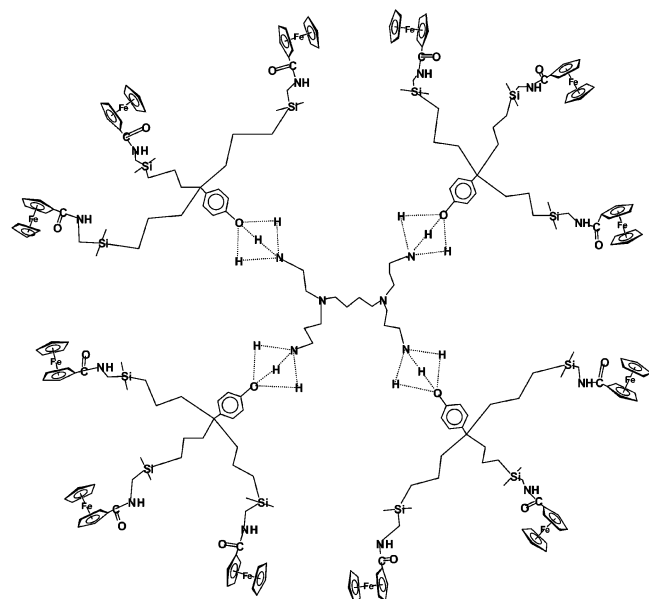


Figure 3. Schematic representation of DAB-12Fc formed with $\text{G}_1\text{-DAB-dend-(NH}_2\text{)}_4$ and dendron **2**.

ferrocenyl dendrimers $\text{G}_n\text{-DAB-}3_x\text{Fc}$ has been monitored by cyclic voltammetry showing the reversible ferrocenyl/ferrocenium system. This addition provokes the decrease of this initial ferrocenyl wave near 0.750 V vs Ag/AgCl and the concomitant increase of a new wave of low intensity (4 times less intense for G_1 and G_2) at a potential less anodic by 250–

280 mV. The tris-amidoferrocenyl-phenol dendron was also used alone in the absence of DAB dendrimer to serve as a reference to evaluate the dendritic effect. With this dendron alone, the addition of $[\text{H}_2\text{PO}_4][n\text{-Bu}_4\text{N}]$ also provokes the appearance of the new wave at a potential 205 mV less anodic than that of the initial wave, whereas this difference is 250 mV with $\text{G}_1\text{-DAB-12Fc}$ and 280 mV with the other supramolecular dendrimers of higher generations $\text{G}_2\text{–G}_5$ (Table 1). Unusual observed features are (i) the dramatically sudden disappearance of the initial wave between 0.4 and 0.5 equiv $[\text{H}_2\text{PO}_4][n\text{-Bu}_4\text{N}]$ for $\text{G}_1\text{-DAB-12Fc}$ and for $\text{G}_2\text{-DAB-24Fc}$, and (ii) the stoichiometry of 0.5 equiv $[\text{H}_2\text{PO}_4][n\text{-Bu}_4\text{N}]$ at the equivalence point for $\text{G}_1\text{-DAB-12Fc}$ (Figure 7). This equivalence point varies with the generation number, however. It increases until G_3 : 0.8 equiv for $\text{G}_2\text{-DAB-24Fc}$ and 1.85 equiv for $\text{G}_3\text{-DAB-48Fc}$, then decreases for the highest generations: 1.70 equiv for $\text{G}_4\text{-DAB-96Fc}$ and 0.95 equiv for $\text{G}_5\text{-DAB-192Fc}$. Finally, the new wave is not electrochemically reversible as indicated by the difference of potential ΔE_p between the anodic and cathodic peaks that is larger than 58 mV, i.e. between 90 and 140 mV, depending on the generation. These features allow titration of $[\text{H}_2\text{PO}_4][n\text{-Bu}_4\text{N}]$ using the supramolecular dendrimers by plotting the decrease of intensity of the initial wave and the increase of intensity of the new wave as a function of the number of equiv $[\text{H}_2\text{PO}_4][n\text{-Bu}_4\text{N}]$ by ferrocenyl branch, and Figure 8 shows an example of such a titration using $\text{G}_2\text{-DAB-24Fc}$.

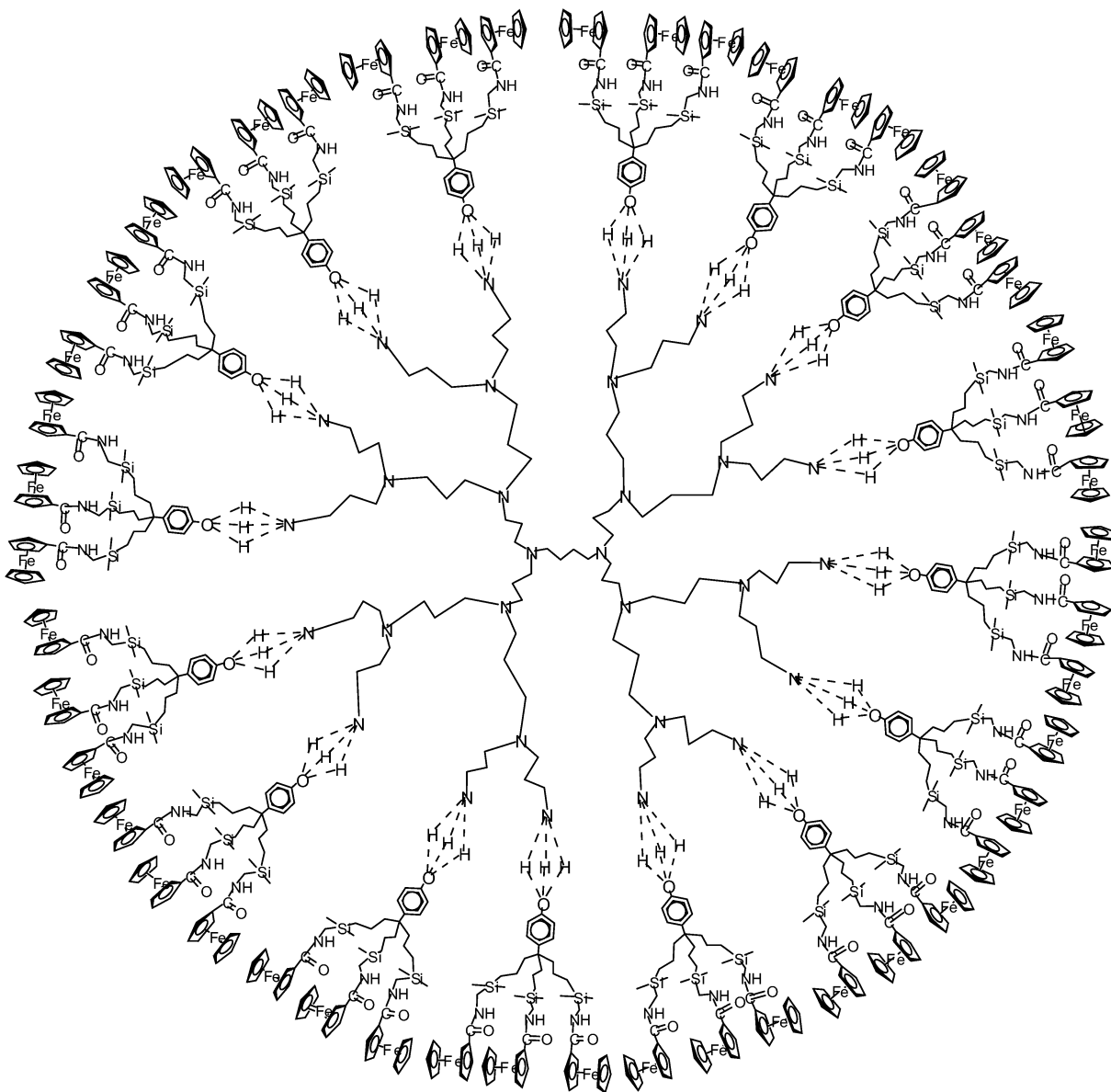


Figure 4. Schematic representation of DAB-48Fc formed with G₃-DAB-dend-(NH₂)₁₆ and dendron 2.

The Kaifer–Echegoyen model (square-scheme)¹⁵ distinguishes the case of a strong interaction between the host and the guest reflected by the appearance of the new CV wave and the case of a weak interaction reflected by a shift of the initial CV wave. Since we are in the first case, the ratio of apparent association constants K_+/K_0 can be estimated as follows: $E^0_1 - E^0_2 = 0.058 \log(K_+/K_0)$ (at 20 °C). The CV waves are chemically reversible, thus the $E_{1/2}$ values deduced from the average of the anodic and cathodic peak potentials are a good approximation of the standard potentials E^0 , which yields K_+/K_0 values of $20\,400 \pm 400$ for G₁ and $67\,000 \pm 3000$ for G₂ to G₅.

ATP²⁻. The interaction of ATP²⁻ with the supramolecular amidoferrocenyldendrimers is of the same type as that with H₂PO₄⁻, i.e., addition of [ATP][*n*-Bu₄N]₂ to a solution of dendrimer provokes the decrease of the initial CV wave and

the appearance of a new wave at less positive potential than that of the initial wave. In terms of the above square scheme, the interaction is again classified as relatively strong, and the K_+/K_0 values are accessible. The new wave shows an electrochemical irreversibility comparable to that observed with H₂PO₄⁻, since the ΔE_p values are of the same order as with H₂PO₄⁻ (Table 2). This new wave also has an intensity lower than that of the initial wave.

There are a few differences, however, between the case of H₂PO₄⁻ and that of ATP²⁻. (i) First, the difference of potentials between the new wave and the initial wave is smaller with [ATP][*n*-Bu₄N]₂ than with [H₂PO₄][*n*-Bu₄N], since, for instance, it varies from 200 mV for G₁-DAB-12Fc to 180 mV for G₅-DAB-192Fc (Figure 9). Whereas a positive dendritic effect was observed with [H₂PO₄][*n*-Bu₄N], the CV experiments with [ATP][*n*-Bu₄N]₂ show a slightly negative dendritic effect. (ii) Then, the drop of intensity of the new wave compared to the initial wave is less marked for ATP²⁻

(15) Seminal report: Miller, S. R.; Gustowski, D. A.; Chen, Z.-H.; Gokel, G. W.; Echegoyen, L.; Kaifer, A. E. *Anal. Chem.* **1988**, *60*, 2021.

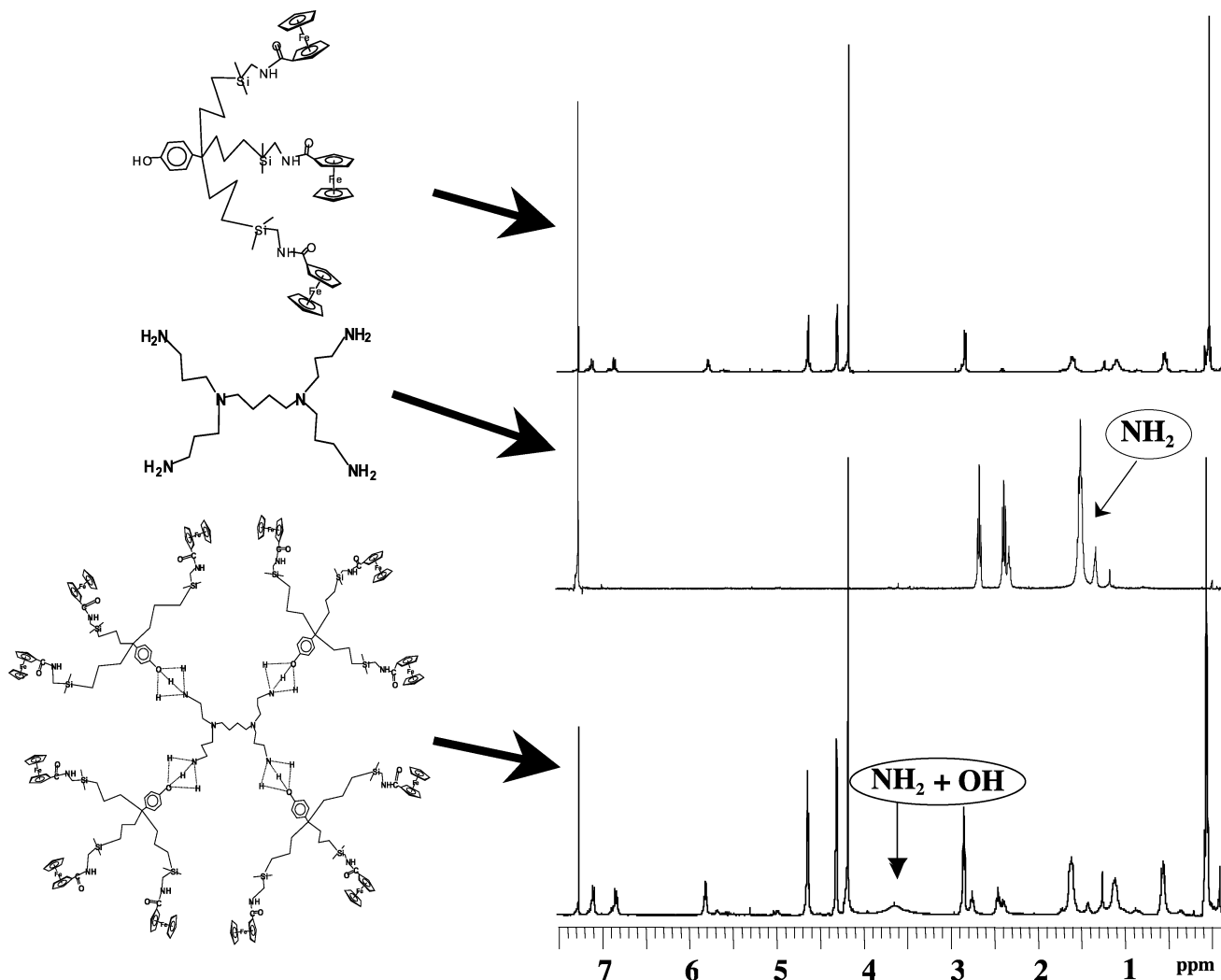


Figure 5. ^1H NMR spectra (400 MHz) of dendron 2, $\text{G}_1\text{-DAB-dend-(NH}_2)_4$, and of their assembly by hydrogen bonds.

than for H_2PO_4^- (Figure 10), but this phenomenon is still present for all the dendrimer generations from G_1 to G_5 . (iii) Finally, the equivalence point is found before 0.5 equiv ATP^{2-} per ferrocenyl branch (from 0.35 equiv $[\text{ATP}][n\text{-Bu}_4\text{N}]_2$ for $\text{G}_1\text{-DAB-12Fc}$ to 0.45 equiv $[\text{ATP}][n\text{-Bu}_4\text{N}]_2$ for $\text{G}_5\text{-DAB-192Fc}$).

No adsorption is found with $[\text{ATP}][n\text{-Bu}_4\text{N}]_2$, even for the highest dendrimer generations. On the other hand, the new wave loses its chemical reversibility beyond the equivalence point, i.e. when more than 0.5 equiv $[\text{ATP}][n\text{-Bu}_4\text{N}]_2$ has been added to the electrochemical cell. Finally, the new wave has a peculiar shape, since its cathodic part contains two waves, although this phenomenon is only clearly observed before the equivalence point is reached. When one equiv $[\text{ATP}][n\text{-Bu}_4\text{N}]_2$ per ferrocenyl branch has been added, only a single cathodic wave is observed.

Discussion

The binding constants between amines and phenols are low, of the order of 40 to 90 L mol^{-1} .^{5c} Such orders of magnitude correspond to relatively weak and reversible hydrogen bonding (ΔH° of the order of 40 kJ/mol). The ^1H NMR data show that the hydrogen-bonding exchange is fast

on the ^1H NMR time scale, since only a concentration-dependent average location of the signal of the overall H-bonded atoms is found. Thus, the dendrons around the central DAB dendrimers should be viewed in a dynamic exchange between free and H-bonded phenol dendrons. The electrochemical time scale of cyclic voltammetry (of the order of 0.1 s) is much larger than that of NMR (of the order of 10^{-8} s), therefore an average situation between the free and hydrogen-bonded states is also observed using this electrochemical technique. The unicity of the ferrocenyl dendrimer wave in cyclic voltammetry is a common feature for all ferrocenyl dendrimers¹⁶ for which the number of atoms between the ferrocenyl centers is large enough to make the electrostatic factor very small.¹⁷ In the present case, there are 11 atoms between the ferrocenyl centers, and the CV wave of the supramolecular dendrimers in CH_2Cl_2 shows the characteristics of a classic ferrocenyl wave without perturbation by the electrostatic factor. The electrochemical

(16) For reviews of ferrocenyl dendrimers and their electrochemistry, see (a) Kaifer, A. E.; Gomez-Kaifer, M. *Supramolecular Electrochemistry*; Wiley-VCH: Weinheim, 1999; Chapter 16, p 207. Casado, C. M.; Cuadrado, M.; Moran, M.; Alonso, B.; Garcia, B.; Gonzales, J.; Losada, J. *Coord. Chem. Rev.* **1999**, 185/186, 53.

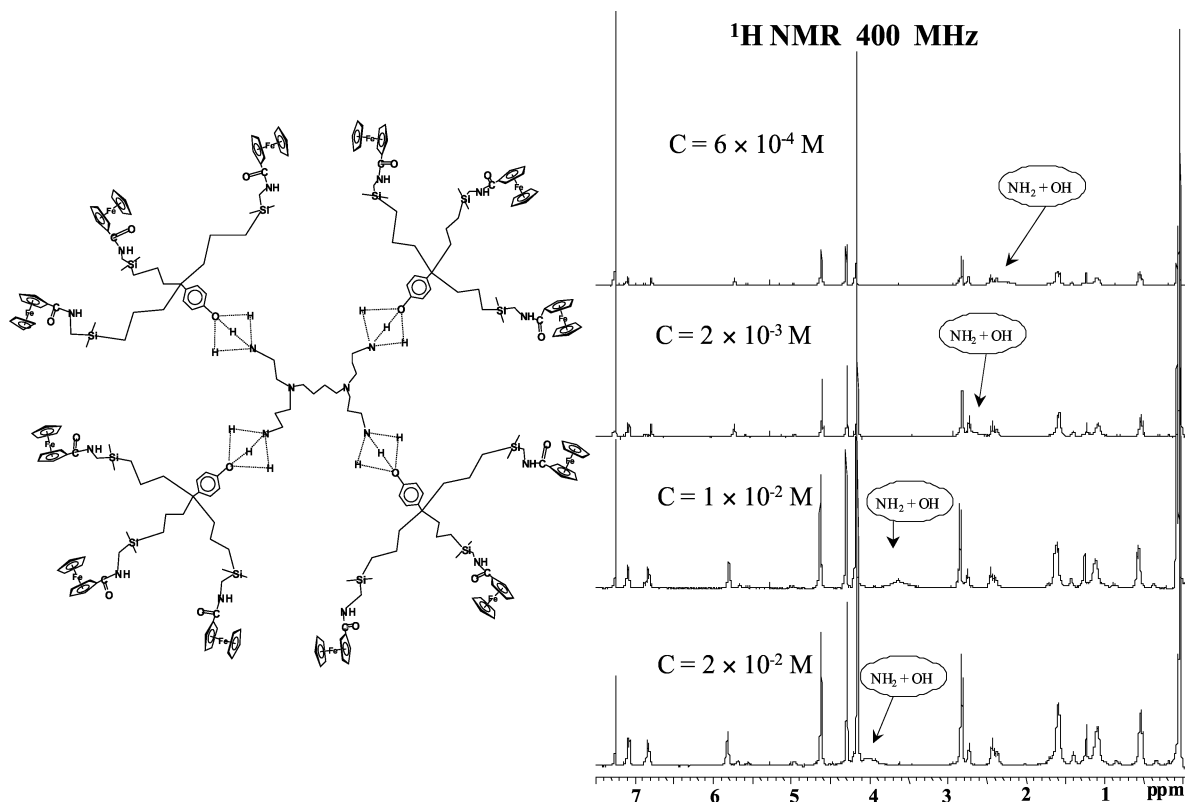


Figure 6. ^1H NMR spectra (400 MHz) of DAB-12Fc in CDCl_3 at different concentrations.

Table 1. Cyclic Voltammetry Data of Dendron **2** and G_n -DAB-3xFc ($x = 2^{n+1}$, $n = 1-5$) Before and During the Titration of H_2PO_4^- in CH_2Cl_2

	$E_{1/2}$ (free) ^a (mV)	ΔE_p (free) ^b (mV)	H_2PO_4^-			I_{final}/I_0^d	saturation (equiv H_2PO_4^-)
			$\Delta E_{1/2}$ (mV)	ΔE_p (mV)	K_+/K_0^c		
Dendron 2	750	55	205	115	3400 ± 100	0.5	1
G_1 -DAB-12-Fc	725	60	250	90	$20\,400 \pm 400$	0.25	0.50
G_2 -DAB-24-Fc	780	55	280	90	$67\,000 \pm 3000$	0.25	0.80
G_3 -DAB-48-Fc	785	55	280	140	$67\,000 \pm 3000$	1	1.85
G_4 -DAB-96-Fc	745	55	280	110	$67\,000 \pm 3000$	0.8	1.50
G_5 -DAB-192-Fc	745	45	280	115	$67\,000 \pm 3000$	0.66	0.95

^a $E_{1/2} = (E_{\text{pa}} + E_{\text{pc}})/2$ vs Ag/AgCl in mV; supporting electrolyte $[n\text{-Bu}_4\text{N}][\text{PF}_6]$ 0.1 M; working electrode and auxiliary electrode Pt; reference electrode Ag; scan rate 200 mV/s; 20 °C. ^b $\Delta E_p = E_{\text{pa}} - E_{\text{pc}}$ in E_{pa} is the anodic peak potential and E_{pc} is the one of cathodic peak. ^c $\Delta E_{1/2} = 0.058 \log(K_+/K_0)$ at 20 °C according to ref 15. ^d I_{final} = intensity of the new wave at saturation; I_0 = intensity of the initial wave before the addition of anion.

Table 2. Cyclic Voltammetry Data of Dendron **2** and G_n -DAB-3xFc Before and During the Titration of ATP^{2-} in CH_2Cl_2

	ΔE_p (free) (mV) ^a	ATP^{2-}			I_{final}/I_0^c	saturation (equiv ATP^{2-})
		$\Delta E_{1/2}$ (mV)	ΔE_p (mV)	K_+/K_0^b		
Dendron 2	55	200	115	2800 ± 100	0.40	0.5
G_1 -DAB-12-Fc	60	200	120	2800 ± 100	0.35	0.36
G_2 -DAB-24-Fc	55	200	130	2800 ± 100	0.46	0.40
G_3 -DAB-48-Fc	55	180	115	1270 ± 40	0.53	0.35
G_4 -DAB-96-Fc	55	180	120	1270 ± 40	0.47	0.45
G_5 -DAB-192-Fc	45	180	115	1270 ± 40	0.47	0.35

^a $\Delta E_p = E_{\text{pa}} - E_{\text{pc}}$, with E_{pa} being the anodic peak potential and E_{pc} being the potential of the cathodic peak. ^b $\Delta E_{1/2} = 0.058 \log(K_+/K_0)$ at 20 °C according to ref 15. ^c I_{final} = intensity of the new wave at saturation; I_0 = intensity of the initial wave before the anion addition.

reversibility is remarkable, especially for the largest ferrocenyl dendrimers for which a static view indicates that a large number of ferrocenyl groups are far from the electrode.

This reversibility implies, however, that rotation of the dendrimers is fast on the electrochemical time scale, since the electron-hopping mechanism among the ferrocenyl units that are far away from one another is expected to be much less efficient in solution than in the solid state.¹⁸

The Kaifer–Echegoyen model of square scheme allows

(17) (a) Bard, A. J.; Faulkner, L. R. *Electrochemical Methods*; Wiley: New York, 1980. (b) Astruc, D. *Electron-Transfer and Radical Processes in Transition-Metal Chemistry*; VCH: New York, 1995; Ch. 2 and 7. (c) Astruc, D. In *Vol. 2 Organic, Inorganic, and Organometallic Molecules* (Mattay, J., Astruc, D., Eds.; Ch. 4, p 728) of *Electron Transfer in Chemistry*; Balzani, V., Ed.; Wiley-VCH: New York, 2001.

(18) Gorman, C. B.; Smith, J. C.; Hager, M. W.; Parkhurst, B. L.; Sierzputowska-Gracz, H.; Haney, C. A. *J. Am. Chem. Soc.* **1999**, *121*, 9958.

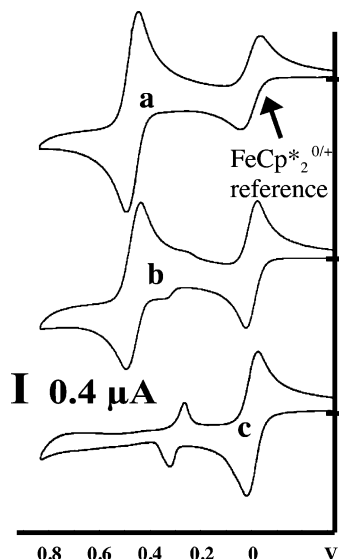


Figure 7. Titration of G₁-DAB-12Fc in CH₂Cl₂ (Pt, [n-Bu₄N][PF₆] 0.1 M, 20 °C, reference FeCp*₂ = decamethylferrocene) with [n-Bu₄N][H₂PO₄]: cyclic voltammogram (a) before the addition; (b) with 0.4 equiv of anion; and (c) with 0.5 equiv of anion.

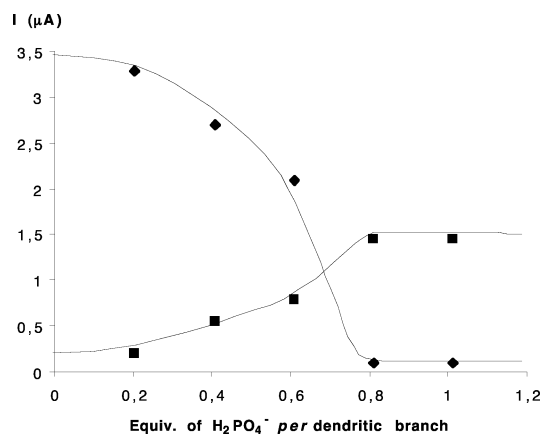


Figure 8. Titration of G₂-DAB-24Fc in CH₂Cl₂ (Pt, [n-Bu₄N][PF₆] 0.1 M, 20 °C, reference FeCp*₂ = decamethylferrocene) with [n-Bu₄N][H₂PO₄]: variation of intensities of initial anodic peak (◆) and new anodic peak (■) during the titration.

rationalizing the electrochemical responses to the recognition phenomena.¹⁵ With amidoferrocenyl dendrimers, it has been established that the interaction is of the relatively strong type with the H₂PO₄⁻ anion. More precisely, this is the case if the synergy between the double hydrogen bonding between the ferrocenylamido group and the H₂PO₄⁻ anion and the electrostatic effect is accompanied by a topological factor either in endo-receptors as shown by Beer's group² or by exo-receptors as indicated in our previous reports.³

The advantage of supramolecular dendrimers is that they do provide this effect even though the dendritic architecture is just formed by simple assembly rather than by tedious dendritic syntheses. Moreover, the positive dendritic effect found for H₂PO₄⁻ enhances the advantage of the use of dendrimers and illustrates the importance of the topological factor. This positive dendritic effect can be rationalized in terms of the decrease of the inter-branch space as the generation number increases, so that the anions are more

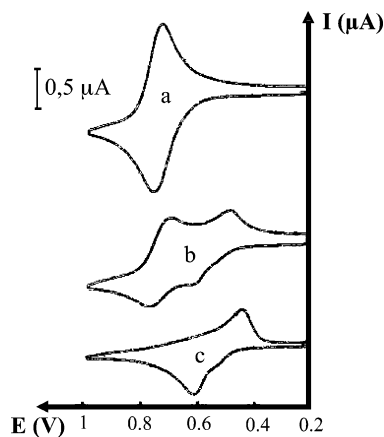


Figure 9. Titration of G₄-DAB-192Fc in CH₂Cl₂ (Pt, [n-Bu₄N][PF₆] 0.1 M, 20 °C, reference FeCp*₂, not shown) with [n-Bu₄N]₂[ATP]: cyclovoltammogram (a) before the addition, (b) with 0.26 equiv of anion; and (c) with 0.35 equiv of anion.

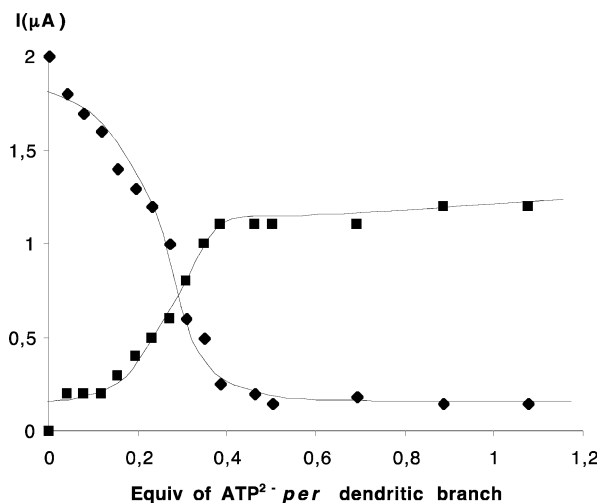


Figure 10. Titration of G₂-DAB-24Fc in CH₂Cl₂ (Pt, [n-Bu₄N][PF₆] 0.1 M, 20 °C, reference FeCp*₂). Variation of intensity of the initial anodic peak (◆) and new anodic peak (■) during the titration.

strongly trapped and bound in narrower channels than in largely open ones.

The remarkable events noted upon reaching the equivalence point in the case of G₁ and G₂ are new and specific to these supramolecular dendrimers. Indeed, we believe that the combination between the 0.5 stoichiometry for G₁ and G₂ and the sudden intensity drop indicates the formation of a large supramolecular assembly in which each anion links two amidoferrocenyl groups. The drop of intensity *i* of the CV wave after the equivalent point indicates that the diffusion coefficient *D* becomes smaller after the equivalence point than before, according to the Sevcik–Randles equation:¹⁷ $i = kAn^{3/2}D^{1/2}v^{1/2}c$, where *A* is the electrode area, *k* is a constant, *n* is the number of electron(s) involved in the redox process, *v* is the scan rate, and *c* is the substrate concentration. The coefficient *D* is related to the size of the electroactive system, thus a drop of *D* means a large size increase. Before the equivalence point, the triferrocenylphenol dendrons are in equilibrium with their dendritic assembly. The intensity of the CV wave represents an average between the free state and the bound state of the triferrocenylphenol

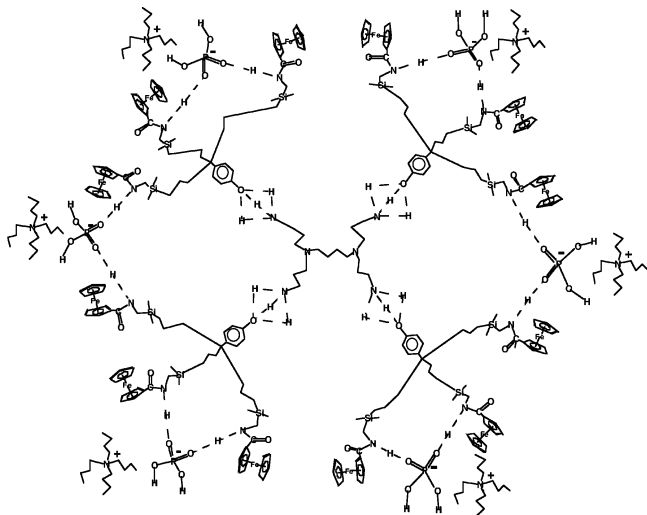


Figure 11. Schematic representation of DAB-12Fc + 0.5 equiv of H_2PO_4^- per dendritic branch. The above representation with 4 16-membered rings and 2 43-membered rings is arbitrary, and an alternative one involving 2 16-membered rings and 4 43-membered ring is also possible, although less entropically favored.

dendrons, because the hydrogen-bonding exchange is much faster than the electrochemical time scale. After the equivalent point, one can speculate that the dendritic assembly is not only larger due to the presence of the $[\text{H}_2\text{PO}_4^-][n\text{-Bu}_4\text{N}]$ species at the periphery of the assembly, but also blocked by the linking H_2PO_4^- groups so that the dendrons can no longer dissociate from the polyamine core (Figure 11). An additional argument along this line is the fact that the DAB-polyamine dendrimers passivate the electrode before the equivalence point, but not after the equivalence point as indicated by the variation of shape of the decamethylferrocene CV wave.

For the highest generation, however, saturation intervenes (beyond G_2) because there is presumably no advantage beyond the ideal situation in the G_2 -DAB-24Fc. Large supramolecular dendrimers might tend to dissociate more readily than the first two-generation ones due to steric effects, and also they more readily adsorb onto the electrode when they bind H_2PO_4^- . Under such conditions, the interaction between the added anion and the dendritic polyamino core may become important and even predominant. This is most probably why such a large amount of equiv anion is necessary to reach the equivalent point with the large DAB polyamine generations G_3 and G_4 . It is also noteworthy that, from the generation G_3 on, the ratio of intensity I_{final}/I_0 becomes of the order of unity or slightly below, meaning that the phenomenon of intramolecular hydrogen bonding suggested for the first generation is no longer significantly involved. It is more likely that the anion interacts with the triferrocenyl dendron whose hydrogen bonding with the dendritic polyamine core is weaker than for G_1 . In this respect, the dendritic effect on the efficiency of the intramolecular process depicted for G_1 is a negative one.

Finally, the electrochemical irreversibility observed after the equivalence point means that the electron transfer from the ferrocenyl state to the ferrocenium state is accompanied by an important structural reorganization of the supramo-

lecular assembly, because the large change in the charge strongly perturbs the hydrogen bonding that in turn strongly influences the overall molecular organization of the assembly.

There are only a few reports of the electrochemical recognition of ATP^{2-} , and the results are subjected to very variable stoichiometries.¹⁰ In the present case, the remarkable aspect is that the electrochemical recognition of ATP^{2-} follows the relatively strong-case type of interaction, which allows its recognition with access to the K_+/K_0 ratio and titration. The difference of potential between the new wave and the initial wave is almost as important as with the H_2PO_4^- anion. However, the events discussed above for H_2PO_4^- are less marked, the stoichiometries are systematically slightly lower than 0.5 and the dendritic effects are weak. These later aspects indicate that the steric effects are responsible for a less sharp and less specific signature of each supramolecular dendrimer with the ATP^{2-} than with the H_2PO_4^- anion. The slightly negative dendritic effect in terms of difference of potential between the initial CV wave and the new wave could signify that the inter-branch space becomes a bit too small for facile insertion of ATP^{2-} in the largest dendrimers. It is also well possible that ATP interacts intermolecularly with two dendrimers forming oligomeric hydrogen-bonded assemblies.

The double negative charge of ATP^{2-} induces some double binding of amidoferrocenyl groups,¹⁹ inducing the formation and electrochemical detection of a mixture of ATP^{2-} bound to one- and two-ferrocenyl units that do not appear at the same potential. Indeed, due to the close proximity of the two ferrocenyl units, the electrostatic factor in the mixed valence system is no longer negligible, causing splitting of the ferrocenyl wave of the doubly bound ATP^{2-} .²⁰ This problem disappears in the presence of excess ATP^{2-} beyond the equivalence point, since the stoichiometry then largely favors single ferrocenyl bonding. The progressive loss of chemical reversibility beyond the equivalence point could be due to the decomposition of amidoferrocenium species in the presence of excess ATP^{2-} anions. Finally, let us recall all studies in the present work were in CH_2Cl_2 , and the detection of ATP^{2-} in water, its natural medium, is considerably more difficult than in organic solvents.

Concluding Remarks

Supramolecular dendrimers involving fast, reversible hydrogen bonding have been assembled by simply mixing commercial DSM polyamine dendrimers and triallyl- or tris-amidoferrocenyl phenol dendrons as shown by the equivalence and new location of the three $\text{NH}_2 + \text{OH}$ protons in the 400 MHz ^1H NMR spectra.

These supramolecular ferrocenyl dendrimers disclose the classic single reversible ferrocenyl/ferrocenium wave in

(19) For the electrochemistry of dinuclear systems, see (a) Taube, H. *Electron Transfer Reactions of Complex Ions in Solution*; Academic Press: New York, 1970. (b) *Mixed Valency Systems. Applications in Chemistry, Physics and Biology*; NATO ASI Series, Vol. C 343; Prasad, K.; Ed.; Kluwer: Dordrecht, 1991. (c) Astruc, D. *Acc. Chem. Res.* **2000**, *33*, 287.

(20) Cuadrado, I.; Casado, C. M.; Alonso, B.; Moran, M.; Losada, J.; Belsky, V. *J. Am. Chem. Soc.* **1997**, *119*, 7613.

cyclic voltammetry due to the weakness of the electrostatic factor. They can be used to recognize and titrate the H_2PO_4^- and ATP^{2-} anions due to the appearance of a new wave at less anodic potentials than the initial wave indicating a strong interaction. The electrochemical recognition is observed with a positive dendritic effect in the difference of potential between the initial CV wave and the new one for H_2PO_4^- and a slightly negative dendritic effect for ATP^{2-} .

New trends in this titration of H_2PO_4^- specific to these supramolecular dendrimers are the dramatically sudden drop of intensity of the CV wave and the 0.5 stoichiometry at the equivalence point observed for G_1 and G_2 . They indicate the formation of a supramolecular assembly around which each of the H_2PO_4^- anions links two amidoferrocenyl groups. These trends are also found for ATP^{2-} , but are less marked than with the H_2PO_4^- anion. With ATP^{2-} , two cathodic CV waves are observed during the titration reflecting the close binding of two ferrocenyl centers to two phosphate groups of ATP^{2-} with electrostatic effect between the ferrocenyl centers. Overall, the results obtained for ATP^{2-} with G_1 and G_2 are of the same magnitude as with the dendron **2** itself. The higher generations of supramolecular dendrimers clearly suffer from steric constraints and/or preferential binding of ATP^{2-} with the DAB dendrimers.

Experimental Section

General Data. Dichloromethane was distilled from calcium hydride just before use. DSM polyamines G_n -DAB-dend-(NH_2)_x were purchased from Aldrich and used as received. ^1H NMR spectra were recorded with a Bruker AC 400 (400 MHz) spectrometer. All chemical shifts are reported in parts per million (δ , ppm) with reference to the solvent or Me_4Si . Cyclic voltammetry data were recorded with a PAR 273 potentiostat galvanostat. Care was taken in the CV experiments to minimize the effects of the solution resistance on the measurements of potentials peaks (the use of positive feedback IR compensation and dilute solution ($\approx 10^{-4}$ mol/L) maintained currents between 1 and 10 μA). The reference electrode was an Ag quasi-reference electrode (QRE). The QRE potential was calibrated by adding the reference couple $[\text{FeCp}_2^*]/[\text{FeCp}_2^{*\dagger}]$. The working electrode (platinum) was treated by immersion in 0.1 M HNO_3 then polished before use and between each recording if necessary. The synthesis of the dendrons **1** and **2** were carried out as reported in refs 14 and 3d, respectively.

Preparation of the Supramolecular Assembly $\{\text{G}_1\text{-DAB-dend-(NH}_2\text{)}_4 + \text{Dendron 2}\}$. A 2.25 mg portion (7.11×10^{-6} mol) of the commercial DSM polyamine $\text{G}_1\text{-DAB-dend-(NH}_2\text{)}_4$ was weighed in an NMR tube with a microbalance and dissolved in 0.6 mL of CDCl_3 . Then, 32.17 mg (4 eq, 28.43×10^{-6} mol) of dendron **2** was weighed and transferred into an NMR tube with 0.6 mL of CDCl_3 . The formation of the supramolecular assembly was observed by ^1H NMR spectroscopy. Spectra of each product were recorded before and after mixing. Then, the solvent was removed and the assembly was dissolved in CH_2Cl_2 and adjusted to 25 mL in a volumetric flask.

^1H NMR (400 MHz, CDCl_3 , δ , ppm): 0.05 (s, 72H, $(\text{CH}_3)_2\text{Si}$); 0.55 (t, 24H, CH_2Si); 1.10 (br, 24H, $\text{CH}_2\text{CH}_2\text{Si}$); 1.40 (br, 4H, $\text{CH}_2\text{-CH}_2\text{N}$ central); 1.58–1.61 (m, 12H, $\text{CH}_2\text{CH}_2\text{NH}_2$ and $\text{ArC}(\text{CH}_2)_3$); 2.43 (m, 12H, CH_2NCH_2); 2.72 (t, 8H, CH_2NH_2); 2.84 (d, 24H, SiCH_2N); 3.11 (br, 12H, $\text{NH}_2 + \text{OH}$); 4.17 (s, 60H, Cp); 4.30 (s, 24H, $\text{C}_5\text{H}_4\text{CO}$); 4.64 (s, 24H, $\text{C}_5\text{H}_4\text{CO}$); 5.81 (t, 12H, NHCO); 6.83 (d, 8H, Ar); 7.10 (d, 8H, Ar).

The formation of supramolecular dendrimers with the other four generations of the DSM dendrimers was carried out as described above.

DAB-24-Fc. ^1H NMR (400 MHz, CDCl_3 , δ , ppm): 0.05 (s, 144H, $(\text{CH}_3)_2\text{Si}$); 0.55 (t, 48H, CH_2Si); 1.10 (br, 48H, $\text{CH}_2\text{CH}_2\text{Si}$); 1.38 (br, 4H, $\text{CH}_2\text{CH}_2\text{N}$ central); 1.58–1.61 (m, 72H, $\text{CH}_2\text{CH}_2\text{-NH}_2$ and $\text{ArC}(\text{CH}_2)_3$); 2.42 (m, 36H, CH_2NCH_2); 2.72 (t, 16H, $\text{CH}_2\text{-NH}_2$); 2.84 (d, 48H, SiCH_2N); 3.19 (br, 24H, $\text{NH}_2 + \text{OH}$); 4.17 (s, 120H, Cp); 4.30 (s, 48H, $\text{C}_5\text{H}_4\text{CO}$); 4.64 (s, 48H, $\text{C}_5\text{H}_4\text{CO}$); 5.82 (t, 24H, NHCO); 6.83 (d, 16H, Ar); 7.10 (d, 16H, Ar).

DAB-48-Fc. ^1H NMR (400 MHz, CDCl_3 , δ , ppm): 0.05 (s, 288H, $(\text{CH}_3)_2\text{Si}$); 0.55 (t, 96H, CH_2Si); 1.10 (br, 96H, $\text{CH}_2\text{CH}_2\text{Si}$); 1.38 (br, 4H, $\text{CH}_2\text{CH}_2\text{N}$ central); 1.58 (m, 152H, $\text{CH}_2\text{CH}_2\text{NH}_2$ and $\text{ArC}(\text{CH}_2)_3$); 2.41 (m, 88H, CH_2NCH_2); 2.72 (t, 32H, CH_2NH_2); 2.84 (d, 96H, SiCH_2N); 3.02 (br, 48H, $\text{NH}_2 + \text{OH}$); 4.17 (s, 240H, Cp); 4.30 (s, 96H, $\text{C}_5\text{H}_4\text{CO}$); 4.64 (s, 96H, $\text{C}_5\text{H}_4\text{CO}$); 5.82 (t, 48H, NHCO); 6.83 (d, 32H, Ar); 7.10 (d, 32H, Ar).

DAB-96-Fc. ^1H NMR (400 MHz, CDCl_3 , δ , ppm): 0.04 (s, 576H, $(\text{CH}_3)_2\text{Si}$); 0.55 (t, 192H, CH_2Si); 1.10 (br, 192H, $\text{CH}_2\text{CH}_2\text{-Si}$); 1.59 (m, 316H, $\text{CH}_2\text{CH}_2\text{NH}_2 + \text{CH}_2\text{CH}_2\text{N}$ central and $\text{ArC}(\text{CH}_2)_3$); 2.41 (m, 180H, CH_2NCH_2); 2.68 (t, 64H, CH_2NH_2); 2.84 (d, 192H, SiCH_2N); 3.05 (br, 96H, $\text{NH}_2 + \text{OH}$); 4.17 (s, 480H, Cp); 4.30 (s, 192H, $\text{C}_5\text{H}_4\text{CO}$); 4.63 (s, 192H, $\text{C}_5\text{H}_4\text{CO}$); 5.80 (t, 96H, NHCO); 6.82 (d, 64H, Ar); 7.10 (d, 64H, Ar).

DAB-192-Fc. ^1H NMR (400 MHz, CDCl_3 , δ , ppm): 0.05 (s, 1152H, $(\text{CH}_3)_2\text{Si}$); 0.55 (t, 384H, CH_2Si); 1.10 (br, 384H, $\text{CH}_2\text{-CH}_2\text{Si}$); 1.58 (m, 636H, $\text{CH}_2\text{CH}_2\text{NH}_2 + \text{CH}_2\text{CH}_2\text{N}$ central and $\text{ArC}(\text{CH}_2)_3$); 2.41 (m, 372H, CH_2NCH_2); 2.72 (t, 128H, CH_2NH_2); 2.85 (d, 384H, SiCH_2N); 3.20 (br, 192H, $\text{NH}_2 + \text{OH}$); 4.17 (s, 960H, Cp); 4.30 (s, 384H, $\text{C}_5\text{H}_4\text{CO}$); 4.63 (s, 384H, $\text{C}_5\text{H}_4\text{CO}$); 5.82 (t, 192H, NHCO); 6.84 (d, 128H, Ar); 7.10 (d, 128H, Ar).

Titration using Cyclic Voltammetry: Common Conditions for all the Captions of the Figures. Solvent distilled CH_2Cl_2 ; temperature 20 °C; supporting electrolyte $[\text{n-Bu}_4\text{N}][\text{PF}_6]$ 0.1 M; internal reference FeCp_2^* ; reference electrode Ag; auxiliary and working electrodes Pt; scan rate 0.2 V/s; anion concentration ($[\text{n-Bu}_4\text{N}][\text{H}_2\text{PO}_4^-]$ or $[\text{n-Bu}_4\text{N}]_2[\text{ATP}^{2-}]$) 5×10^{-2} M.

General Method for the Titration of H_2PO_4^- or ATP^{2-} . First, $[\text{n-Bu}_4\text{N}][\text{PF}_6]$ was introduced into the electrochemical cell that contained the working electrode, the reference electrode, and the counter electrode, and it was dissolved in freshly distilled dichloromethane. A blank voltammogram was recorded without dendrimer to check the working electrode. Then, 2 mL of the solution of supramolecular dendrimer in dichloromethane was added into the cell. About 1 mg (3×10^{-6} mol) of decamethylferrocene was also added. After degassing the solution by flushing dinitrogen, the CV of the dendrimer alone was recorded. Then, the anion H_2PO_4^- or ATP^{2-} was added as the $\text{n-Bu}_4\text{N}^+$ salts by small quantities using a microsyringe. After each addition, the solution was degassed, and a CV was recorded. The appearance and progressive increase of a new wave was observed while the initial wave decreased and finally disappeared (see the titration graphs). When the initial wave had completely disappeared, addition of the salt of the anion was continued until reaching twice the volume already introduced.

Acknowledgment. Financial support from the Institut Universitaire de France (IUF, D.A.), the Centre National de la Recherche Scientifique (CNRS), the University Bordeaux I, and the Ministère de la Recherche et de la Technologie (MRT, grant to M.-C.D.) are gratefully acknowledged.

IC0493999